Inorg. Chem. **2004**, *43*, 4272–4277

Lead and Thallium Tetrakis(imidazolyl)borates: Modifying Structure by Varying Metal and Anion

Barton H. Hamilton and Christopher J. Ziegler*

Department of Chemistry, Knight Chemical Laboratory, University of Akron, Akron, Ohio 44325-3601

Received February 16, 2004

We are using the coordinating anions tetrakis(imidazolyl)borate and tetrakis(4-methylimidazolyl)borate to construct new metal–organic framework structures. In this report, we are exploring materials similar in composition to the previously reported layered network structure $Pb[B(Im)_4](NO_3)(nH_2O)$. The metal in this compound can be replaced with isoelectronic Tl(I), affording $Tl[B(Im)_4]$, and the borate can be modified by using 4-methylimidazole, resulting in $Pb[B(4\text{-MeIm})_4](NO_3)$ and $Tl[B(4\text{-MeIm})_4]$. Like the parent $Pb[B(Im)_4](NO_3)(nH_2O)$, $Tl[B(Im)_4]$ and $Tl[B(4\text{-MeIm})_4]$ are layered network structures but both lack anions or solvent molecules in the interlayer spacing. The material $Pb[B(4\text{-MeIm})_4](NO_3)$, however, exhibits a 3D network structure that lacks an open topology, resulting from the increased stereochemical activity (greater steric bulk toward other ligands) of the 4-methylimidazole ring. Both of the Tl(I) solids display longer M–N bonds than observed in the analogous Pb(II) compounds; these lengths account for the decreased effect of the stereochemical activity of the 4-methylimidazole ring in $Tl[B(4\text{-MeIm})_4]$.

Introduction

The design of ordered solids, also known as crystal engineering, continues to be an important subfield of supramolecular chemistry.[1] Over the past decade, a plethora of network systems have been synthesized, with many examples of coordination polymers[2] and metal organic frameworks[3] appearing in the literature. Although the fabrication of crystalline coordination polymers has become somewhat routine, two challenges remain in this field. With the maturation of crystal engineering, the development of functional solids is accelerating,[4] with applications that range from the catalysis of organic transformations[5] to magnetic materials.[6] The second challenge concerns understanding the factors that control topology in network solids.[7] While some advances have been made for certain ligand systems, there is still not a complete understanding of how network structures can be controlled through component selection, reaction stoichiometry, or crystal growth conditions.[1,3a] In addition to theoretical studies, the generation of materials where small parameters have been changed can provide insight into the factors that affect network structure topology.

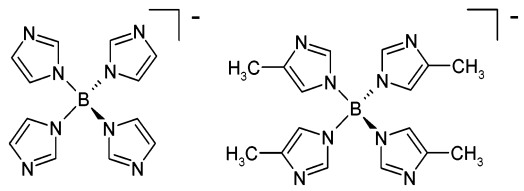

Figure 1. Structures of tetrakis(imidazolyl)borate (BX_4^-, left) and tetrakis-(4-methylimidazolyl)borate (BY_4^-, right).

We have recently presented some of our initial work on network structures incorporating the coordinating anion tetrakis(imidazolyl)borate (Figure 1) and are currently exploring the structural parameter space of solids with this

* Author to whom correspondence should be addressed. E-mail: ziegler@uakron.edu.

(1) *Crystal Design: Structure and Function*; Desiraju, G. R., Ed.; Perspectives in Supramolecular Chemistry; Wiley: West Sussex, U.K., 2003; Vol. 7.
(2) (a) Cernak, J.; Orendac, M.; Potocnak, I.; Chomic, J.; Orendacova, A.; Skorsepa, J.; Feher, A. *Coord. Chem. Rev.* **2002**, *224*, 51−66. (b) Holmes, S. M.; Girolami, G. S. *J. Am. Chem. Soc.* **1999**, *121*, 5593−5594.
(3) (a) Moulton, B.; Zaworotko, M. J. *Chem. Rev.* **2001**, *101*, 1629−1658. (b) Eddaoudi, M.; Moler, D. B.; Li, H. L.; Chen, B. L.; Reineke, T. M.; O'Keeffe, M.; Yaghi, O. M. *Acc. Chem. Res.* **2001**, *34*, 319−330.
(4) Janiak, C. *J. Chem. Soc., Dalton Trans.* **2003**, *14*, 2781−2804.
(5) (a) Xing, B. G.; Choi, M. F.; Xu, B. *Chem.−Eur. J.* **2002**, *8*, 5028−5032. (b) Chui, S. S. Y.; Lo, S. M. F.; Charmant, J. P. H.; Orpen, A. G.; Williams, I. D. *Science* **1999**, *283*, 1148−1150. (c) Forster, P. M.; Cheetham, A. K. *Top. Catal.* **2003**, *24*, 79−86.
(6) (a) Sato, Y.; Ohkoshi, S.; Arai, K.; Tozawa, M.; Hashimoto, K. *J. Am. Chem. Soc.* **2003**, *125*, 14590−14595. (b) Beauvais, L. G.; Long, J. R. *J. Am. Chem. Soc.* **2002**, *124*, 12096−12097.
(7) (a) Desiraju, G. R. *J. Mol Struct.* **2003**, *656*, 5−15. (b) Mitzi, D. B. *J. Chem. Soc., Dalton Trans.* **2001**, 1−12.

10.1021/ic0497984 CCC: $27.50
Published on Web 06/17/2004

species.[8] This synthon is negatively charged, structurally rigid, tetrahedral, and stable to temperatures in excess of 250 °C. Tetrakis(imidazolyl)borate can readily form network solids with metal cations and can afford solids with open or solvent-occupied metal sites. We have previously discussed how the conformations of tetrakis(imidazolyl)borate can contribute to structure in network solids.[8] However, in addition to the rotamers of the borate, several other parameters could affect network connectivity, including the identity of the metal ion and the steric bulk of the organic fragment.

In this report, we are investigating how the identities of the components of a network solid affect its topology. In two earlier publications, we described the layered network solid $Pb[B(Im)_4](NO_3)(nH_2O)$ which can engage in mineral-like behavior and act as a scaffold for organic guests.[9] In this paper, we present three analogues of $Pb[B(Im)_4](NO_3)\cdot nH_2O$ where either the metal and/or the borate have been slightly modified. Upon changing of the metal from Pb to Tl and changing of the borate to the more sterically hindered tetrakis(4-methylimidazolyl)borate, the structures of the metal−borate networks change significantly. Substitution of Tl for Pb both eliminates the need for the nitrate counterion as well as modifies the coordination at the metal center. The replacement of 4-methylimidazole for imidazole on the borate (Figure 1) increases the stereochemical activity of the ligand, which can change the coordination sphere around the metal center and significantly alter the extended network structure. By generating a series of related compounds, we observe that the symmetry about the metal center (holodirected versus hemidirected) in row 6 network solids controls the topology in these materials.

Experimental Section

All reagents and solvents were purchased from Aldrich and used as received. Water was purified by using a Milli-Q Reagent Water System. Elemental analysis was performed at the School of Chemical Sciences Microanalytical Laboratory at the University of Illinois at Urbana-Champaign. Solution NMR spectroscopy was performed on a Varian VXR 300 MHz NMR instrument. Solid-state NMR spectra were obtained on a Varian Unityplus-200 (4.7 T) spectrometer using Doty Scientific supersonic and standard MAS probes. Infrared spectroscopy was carried out on a Bomem MB-100 IR system. Mass spectra were obtained on a Micromass AutoSpec EBEhQ hybrid tandem mass spectrometer using FAB ionization. Sodium tetrakis(imidazolyl)borate was prepared as previously described.[8]

Synthesis of Na[B(4-MeIm)4], 1. The synthesis of this material was based on a procedure developed by Trofimenko for sodium tetrakis(pyrazolyl)borate and is described by Chao and co-workers.[10] Under neat conditions and in an inert nitrogen environment, 10.0 g (0.139 mol) of 4-methylimidazole was melted and stirred in the presence of 1.10 g (0.029 mol) of $NaBH_4$ in a round-bottom flask attached to an oil bubbler. As the heat was slowly increased to about 120 °C, the N_2 flow was stopped, and the H_2 gas evolution was monitored visually by observing the flow through the oil bubbler. Upon reaching 225 °C, H_2 gas generation ceased. The reaction mixture was then cooled to 70 °C, and 200 mL of acetone was added with vigorous mixing. After isolation by vacuum filtration using a fine frit, the product was recrystallized from boiling ethanol and collected. A total of 1.23 g (12%) of the off-yellow product $Na[B(4\text{-}MeIm)_4]$ was recovered. ^1H NMR (D_2O): 2.098, 6.602, 7.218 ppm. ^{13}C NMR: 11.98, 118.55, 137.82, 140.08 ppm. FAB MS (negative ion): *m/z* 335.4, ($B(4\text{-}MeIm)_4^-$). IR (KBr): 3444, 3145, 2918, 2867, 1655, 1568, 1490, 1449, 1383, 1326, 1264, 1233, 1139, 1053, 1007, 976, 940, 821, 765, 677 cm^{-1}.

General Procedure for the Synthesis of Metal Borates. The syntheses of the three variants were based on the synthesis of $Pb[B(Im)_4](NO_3)\cdot nH_2O$ (**2**).[9] A solution of the metal salt (1.0 mmol of metal ion) in 10 mL of deionized water was added to a 1:1 ethanol/water solution (10 mL) of sodium borate salt (1.0 mmol). White, microcrystalline precipitates typically formed immediately or upon minimization of the solution volume, which were then collected by filtration. Large crystals of each material could be grown by slow diffusion of layers of the above two solutions at 60 ° C.

Tl[B(Im)$_4$] (3) was generated using Tl_2SO_4 and $NaB(Im)_4$ with a yield of 83.2 mg (52%). IR (KBr): 3443, 3104, 1631, 1473, 1292, 1261, 1243, 1208, 1109, 1077, 918, 815, 768, 752, 664 cm^{-1}. Solid-State ^{13}C MAS NMR: 123.09, 129.44, 144.44 ppm. Anal. Calcd for $C_{12}H_{12}N_8BTl$: C, 29.81; H, 2.48; N, 23.18. Found: C, 29.56; H, 2.40; N, 22.19.

Pb[B(4-MeIm)$_4$](NO$_3$) (**4**) was generated using $Pb(NO_3)_2$ and **1** with a yield of 17.2 mg (16%). IR (KBr): 3445, 3120, 2926, 1629, 1573, 1527, 1476, 1449, 1384, 1318, 1260, 1229, 1139, 1058, 1041, 1012, 976, 850, 824, 764, 672, 664, cm^{-1}. Solid-State ^{13}C MAS NMR: 12.11, 121.36, 138.67 ppm. Anal. Calcd for $C_{16}H_{20}N_9O_3BPb$: C, 31.79; H, 3.31; N, 20.86. Found: C, 31.77; H, 3.37; N, 20.27.

Tl[B(4-MeIm)$_4$] (5) was generated using Tl_2SO_4 and **1** with a yield of 102 mg (56%). IR (KBr): 3445, 2919, 1633, 1478, 1445, 1383, 1330, 1263, 1232, 1140, 1008, 955, 849, 823, 767, 681, cm^{-1}. Solid-State ^{13}C MAS NMR: 11.14, 14.61, 120.21, 138.10 ppm. Anal. Calcd for $C_{16}H_{20}N_8BTl$: C, 35.62; H, 3.71; N, 20.77. Found: C, 35.48; H, 3.65; N, 20.15.

X-ray crystallography. The X-ray intensity data for compounds **3**−**5** were measured at 100 K (Bruker KRYO-FLEX) on a Bruker SMART APEX CCD-based X-ray diffractometer system equipped with a Mo-target X-ray tube (λ = 0.710 73 Å). The crystals were mounted on cryoloops using Paratone N-Exxon oil and placed under a stream of nitrogen. The detector was placed at a distance of 5.009 cm from the crystal. Frames were collected with a scan width of 0.3° in ω. The frames for each data set were integrated with the Bruker SAINT software package using a narrow-frame integration algorithm. The data were corrected for absorption with the SADABS program. The structure was solved and refined using the Bruker SHELXTL (version 6.1) software package until the final anisotropic full-matrix least-squares refinement on F^2 converged.[11] Experimental details for the three structures are shown in Table 1, and selected bond lengths and angles are listed in Table 2.

Results and Discussion

The reaction of a $Na[B(Im)_4]$ and aqueous $Pb(NO_3)_2$ produces a product with the formula $Pb[B(Im)_4](NO_3)\cdot nH_2O$

(8) Hamilton, B. H.; Kelly, K. A.; Malasi, W.; Ziegler, C. J. *Inorg. Chem.* **2003**, *42*, 3067−3073.

(9) (a) Hamilton, B. H.; Kelly, K. A.; Wagler, T. A.; Espe, M. P.; Ziegler, C. J. *Inorg. Chem.* **2002**, *41*, 4984−4986. (b) Hamilton, B. H.; Kelly, K. A.; Wagler, T. A.; Espe, M. P.; Ziegler, C. J. *Inorg. Chem.* **2004**, *43*, 50−56.

(10) (a) Trofimenko, S. *J. Am. Chem. Soc.* **1967**, *89*, 3170−7. (b) Trofimenko, S. *J. Coord. Chem.* **1972**, *2*, 75−7 (c) Chao, S. M.; Carl, E. *Anal. Chim. Acta* **1978**, *100*, 457−67.

(11) Sheldrick, G. M. *SHELXTL, Crystallographic Software Package*, version 6.10; Bruker-AXS: Madison, WI, 2000.

Table 1. Crystallographic Data Collection and Structure Parameters for Compounds **3**−**5**

	3	**4**	**5**
mol formula	$TlBC_{12}H_{12}N_8$	$PbBC_{16}H_{20}N_9O3$	$TlBC_{16}H_{20}N_8$
fw	483.48	604.41	539.58
space group	$P\bar{1}$	$P4n2$	$P\bar{1}$
a (Å)	8.3541(8)	11.8787(8)	9.2033(9)
b (Å)	8.7948(9)	11.8787(8)	9.7728(9)
c (Å)	10.1676(10)	7.0539(10)	11.2972(10)
α (deg)	92.330(2)	90	79.6080(10)
β (deg)	100.383(2)	90	73.1080(10)
γ (deg)	104.589(2)	90	76.4220(10)
Z	2	2	2
V (Å^3)	708.20(12)	995.33(17)	938.18(15)
T (°C)	−173	−173	−173
λ (Å)	0.710 73	0.710 73	0.710 73
abs coeff μ_{calc} (mm^{-1})	11.41	8.515	8.625
δ_{calc} (Mg/m^3)	2.267	2.017	1.910
$R(F_o)^a$	0.0217	0.0375	0.0158
$R_w(F_o^2)^b$	0.0566	0.0972	0.0381

^{a} $R = \sum||F_o| - |F_c||/\sum|F_o|$. ^{b} $R_w = [\sum w(|F_o^2| - |F_c^2|)^2/\sum w(F_o^2)^2]^{1/2}$.

Table 2. Selected Bond Lengths and Angles for Compounds **2**−**5**

	2	**3**	**4**	**5**
M−N (Å)	2.406(3)	2.573(3)	2.653(5)	2.559(2), 2.647(2), 2.850(2)
	2.505(3)	2.681(3)		2.955(2)
	2.523(4)	2.792(3)		
	2.643(3)	3.241(3)		
N−M−N (deg)	77.09(12)	77.09(9)	81.78(17)	76.01 (7)
	78.30(10)	78.72(9)	98.23(17)	77.91 (7)
	79.03(11	78.86(9)	179.4(6)	80.93(7), 86.64(7)
	80.66(12)	89.69(9)		100.26(7)
	83.86(11)	92.24(9)		151.57(7)
	149.58(11)	155.00(9)		

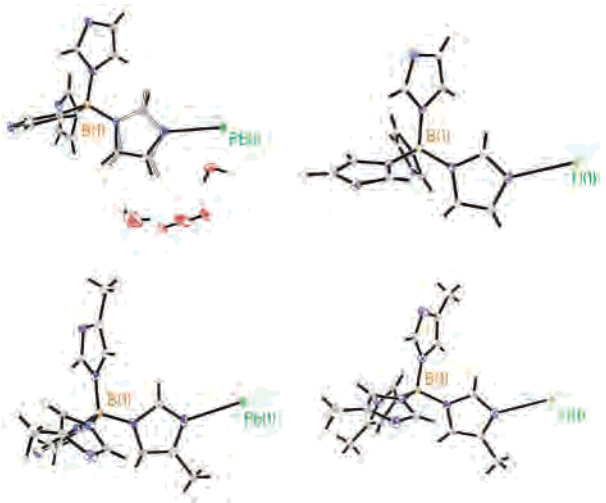

Figure 2. Asymmetric units with 50% thermal ellipsoids of compounds **2** ($Pb[BX_4](NO_3)(nH_2O)$, top left), **3** ($Tl[BX_4]$, top right), and **5** ($Tl[BY_4](NO_3$, bottom right). An extended view of the asymmetric unit of **4** ($Pb[BY_4](NO_3)$) can be seen on the bottom left, showing the full structure of the borate. In **4**, the disordered nitrate has been omitted for clarity.

(**2**), where $n = 0-1.5$. This work has been published previously.[9] Diffusion crystal growth from ethanol/water produces platelike crystals of this material, and the structure of the compound can be readily elucidated by X-ray crystallography. The repeating asymmetric unit of the crystal structure with 50% thermal ellipsoids is shown in Figure 2. In the crystal structure, there are 1.35 waters/asymmetric unit; however, the degree of hydration can vary in the bulk material depending on the extent of water intercalation.[9b]

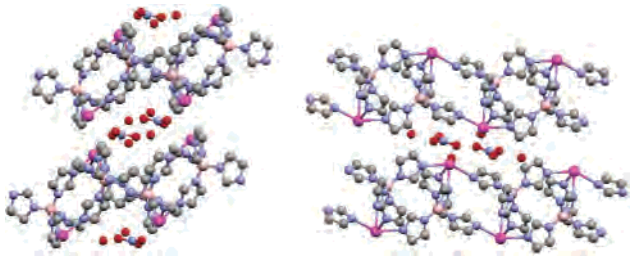

Figure 3. Extended structure of **2** along the c axis (left) and a axis (right). The lead atoms are in purple, and hydrogen atoms have been omitted for clarity.[9a]

One imidazole ring is bound to the metal center in this unit, and the remaining heterocycles are coordinated to different lead sites in adjacent asymmetric units. The nitrate anion, required for charge balance, and the water molecules occupy the void space in the crystal.

In the case of $Pb[B(Im)_4](NO_3)(nH_2O)$, the individual asymmetric units form an extended layered solid, as shown in Figure 3. The metal ions occupy sites at the layer interface, and the borates cross the layer itself. The nitrates and solvent water molecules reside in the void space between the Pb−borate tiers. There are no bonding contacts between the layers that have an approximate spacing of 3.4 Å. Each Pb ion is four coordinate and has a stereochemically active lone pair according to the VSEPR convention. Pb(II) is one of the lower main group elements that exhibits the "inert pair" effect, the lack of participation of the $6s^2$ electrons in covalent bond formation.[12] If this pair of electrons exerts an effect

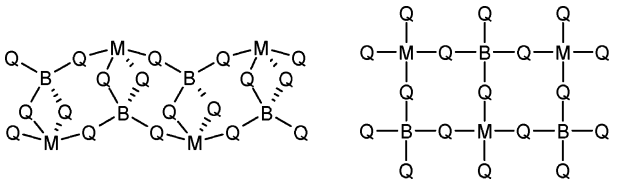

Figure 4. Line illustrations showing the two types of metal−borate connectivity observed in compounds **2**−**5**, where Q is either imidazole (X) or *N*-methylimidazole (Y). The left diagram shows the connectivity observed in compounds **2**, **3**, and **5**, which exhibit asymmetric metal coordination environments bridged by pseudotetrahedral borates. The right diagram shows an axial view of the connectivity in compound **4**, where the tetrahedral borates bridge the square planar metal sites to afford a 3D network structure. The nitrates in compound **2**, **3**, and **5** (and solvent water in **2**) fit above and below the layers, while the disordered nitrates lie along the axial ordinate in **4**.

on the structure at the metal site through nonspherical charge distribution, then an asymmetric geometry results, described as a hemidirrected center. If the inert pair has no effect on metal geometry, then the VSEPR convention fails and a symmetric, holodirected geometry results.

The formation of a layered geometry in **2** is not unexpected, considering the geometry of the metal center and the frequency of this morphology in Pb(II) solid-state structures. For example, the structure of the litharge form of PbO also adopts a layered topology with four-coordinate metal centers.[13] The connectivity forms for two reasons: the asymmetric coordination geometry (square pyramidal) at the metal center; the volume ratios of the borate and Pb(II) cation. The radius ratio for the Pb(II) (1.19 Å)[13] and the borate (boron to external nitrogen distance: ∼5.06 Å) is 0.235, which is indicative of a lower coordination number ranging between 4 and 5 for the metal ion.[14] The asymmetric geometry at the metal allows for the Pb−borate connectivity to close in on itself and form discrete layers. A line diagram displaying this layered metal−borate connectivity is shown in Figure 4. To test these observations on how geometry and radius ratio control structure in **2**, we decided to generate several similar solids where the metal and/or the borate had been modified. With regard to the metal, we chose to make a thallium analogue of **2** to see if the metal radius does contribute to the formation of the layered topology. Monovalent thallium is isolectronic to Pb(II) and can exhibit the inert pair effect. The radius ratio of Tl(I) to tetrakis(imidazolyl)borate is 0.277, which is not much larger than in **2**.[14] Tl(I) can also exhibit asymmetric coordination environments similar to those of Pb(II). However, an analogous thallium borate would not require the presence of a nitrate counterion. In addition to changing the metal, we wanted to determine if the steric bulk of the borate anion could affect the geometry at the metal site.

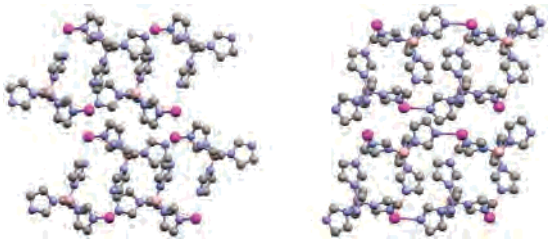

Figure 5. Extended structure of **3** along the *b* axis (left) and along the *ac* plane orthogonal to the *b* axis (right). The thallium atoms are in purple, and hydrogen atoms have been omitted for clarity. The solid lines about the metal ions indicate short coordination bonds (<2.6 Å), and the dashed lines indicate longer coordination bonds (>2.7 Å). The right of the figure corresponds to the left view in Figure 4.

The compounds Tl[B(Im)$_4$] (**3**), Pb[B(4-MeIm)$_4$](NO$_3$) (**4**), and Tl[B(4-MeIm)$_4$] (**5**) were synthesized using conditions identical with those for Pb[B(Im)$_4$](NO$_3$). All three procedures afforded crystalline products and large single crystals that could be investigated using X-ray diffraction methods. The parameters of the three data collections are presented in Table 1, and the structures of the repeating units of the three crystals are shown in Figure 2. Each compound shows an identical stoichiometry of metal to borate as seen in **2**. Compounds **3** and **5** are both triclinic crystals with overall parameters similar to that found in **2**; however, both materials lack a nitrate counterion. Compound **4** is an orthorhombic crystal, and its asymmetric unit contains only one of the four imidazole rings on the borate. However, the stoichiometry of borate, lead, and nitrate in the empirical formula is identical with that of **2**. In the solution of **4**, the nitrate was disordered and was modeled as a diffuse contributor without specific atom positions.

We predicted that the structure of **3** would exhibit a network connectivity similar to that of **2** but without the presence of the nitrate counterion in the interlayer spacing. Inspection of the extended network structure of **3** (Figure 5) does indeed show that it closely resembles that of **2**. The thallium borate units form two-dimensional layers, with the metal sites facing the interlayer spacing. Due to the charge balance between the borate and the Tl(I), there is no need for an additional counterion. As a result, the layers in the solid are closer together than in **2**, and the volume of the asymmetric unit decreases significantly as one goes from **2** (911.84 Å) to **3** (708.20 Å). One important difference between the structures of **2** and **3** is the coordination at the metal; compound **3** has significantly longer metal−ligand bond distances than in **2**. In particular, one imidazole−Tl bond is very long, 3.241(3) Å, which is more than 0.7 Å longer than the average Pb(II)−N bond distance of 2.52 Å in **2** and approaches the nonbonding limit. However, despite these long coordination bonds, the disphenoidal geometry results in a network structure very similar to that observed in **2** and shown on the left side of Figure 4.

While switching from lead to thallium does not change the layered topology, modifying the borate can have a much more significant effect on the network structure. In compound

(12) Shimoni-Livny, L.; Glusker, J. P.; Bock, C. W. *Inorg. Chem.* **1998**, *37*, 1853−1867.
(13) Greenwood, N. N.; Earnshaw, A. *Chemistry of the Elements*; Pergamon Press: Oxford, U.K., 1984.
(14) Wells, A. F. *Structural Inorganic Chemistry*, 5th ed.; Clarendon Press: Oxford, U.K., 1984.

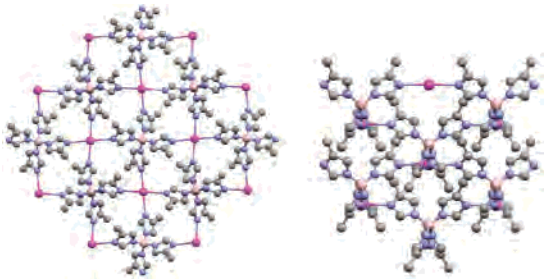

Figure 6. Extended structure of **4** along the *c* axis (left) and *b* axis (right). The lead atoms are in purple, and hydrogen atoms and disordered nitrate have been omitted for clarity. The disordered nitrates lie along the *c* axis in the same lines as the Pb atoms. The left of the figure corresponds to the right view in Figure 4.

4, which contains tetrakis(4-methylimidazolyl)borate, the additional steric bulk affects the geometry around the metal. The environment changes from dispheniodal as in **2** and **3** to a square planar geometry of the imidazole rings in **4**. The metal−ligand bond distance in **4** (2.653(5) Å) is only slightly longer than the average distance in **2**, ∼2.52 Å. Clearly, the steric bulk of the methyl group increases the stereochemical activity of the imidazole ring, widening the adjacent N−Pb−N bonds from an average angle of ∼80° in **2** to ∼90° in **4**. As a result, the structure deviates from the VSEPR prediction, and there is no longer a clear stereochemically active lone pair contributing to the geometry. The axial sites in this structure are occupied by the disordered nitrate, which alternates between a symmetric bidentate and a monodentate coordination mode. The resultant structure is a symmetric, or holodirected, geometry about the metal center.[12] The factors that control symmetric versus asymmetric geometries in Pb(II) compounds are still not understood fully; work continues in the fundamental coordination chemistry of lead.[15]

The change from dispheniodal to square planar affects the network connectivity in compound **4** relative to that observed in **2** and **3**. Figure 6 shows the network structure of compound **4**, and the right side of Figure 4 displays an illustration of the connectivity observed from the axial direction. While the asymmetric geometries at the metal site in **2** and **3** result in the observed layer topologies, the highly symmetric coordination environment in **4** leads to three-dimensional connectivity. The metals line up along the *c* axis bridged by disordered nitrate counterions. The borates link the metal sites in a metal−borate square spiral pattern, exhibiting interlaced enantiomeric helices. Similar coordination modes have been observed in the group II metal imidazolylborates, but in those cases, the borates form closed loops with the metals and result in one-dimensional chains or two-dimensional layers.[8] Due to the closed topology of **4**, this material does not reversibly intercalate water molecules nor does it exhibit ion exchange behavior with other anions, as observed in the layered compound **2**.[9]

(15) (a) Harrowfield, J. M.; Shahverdizadeh, G. H.; Soudi, A. A. *Supramol. Chem.* **2003**, *15*, 367−373. (b) Harrowfield, J. M.; Miyamae, H.; Skelton, B. W.; Soudi, A. A.; White, A. H. *Aust. J. Chem.* **2002**, *55*, 661−666. (c) Harrowfield, J. M.; Skelton, B. W.; White, A. H. *J. Chem. Soc., Dalton Trans.* **1993**, 2011−2016.

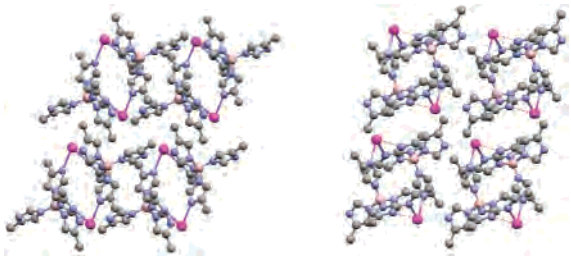

Figure 7. Extended structure of **5** along the *b* axis (left) and *a* axis (right). The thallium atoms are in purple, and hydrogen atoms have been omitted for clarity. The solid lines about the metal ions indicate short coordination bonds (<2.6 Å), and the dashed lines indicate longer coordination bonds (>2.7 Å). The right of the figure corresponds to the left view in Figure 4.

In compound **5**, both the identity of the metal ion has been changed and the structure of the borate has been modified relative to that of species **2**. While we expected that the charge balance in this material would eliminate any additional counterion in the solid, it was unclear what factors would dominate the network connectivity. Thallium prefers lower coordination numbers,[13] which could allow for an asymmetric geometry and a layered topology, but the increased steric bulk of the 4-methyl imidazole ring could compete with the stereochemical activity of the lone pair. Elucidation of the structure of **5** (Figure 7) shows that long M−N bond distance preference for Tl(I) dominates the structure and that this allows for the formation of a layered topology similar to that in **2** and **3**, as shown on the left side of Figure 4. As in **3**, four imidazole rings are coordinated to the metal center but exhibit much longer M−N bond distances than in **2** or **4**. Interestingly, the average bond distance is shorter than in **3**, which implies that crystal packing has a significant effect on the metal−ligand bond lengths in these compounds. The geometry is asymmetric and conforms to VSEPR prediction. Although the N−Tl−N bond angles are larger than those found in **3**, the increased Tl−N bond lengths at the metal center translate into less crowding and a smaller effect of the increased steric bulk of the 4-methylimidazole.

In conclusion, we have begun to explore how the identity of metal ion and bulk of the borate affects a series of $Pb[B(Im)_4](NO_3)$ analogues. Both Pb(II) and Tl(I) in these solids prefer asymmetric geometries, resulting in the observed 2D layered topologies. Increasing the steric bulk of the imidazole ring with a methyl group at the 4 position increases the nitrogen−metal−nitrogen bond angles of the solid. In **4**, this results in a symmetric coordination environment around the metal and a closed 3D network structure. A similar bond angle widening is observed in **5**, but due to the increased metal−ligand bond length, the geometry remains asymmetric and a layered structure results. We are continuing our investigation into control of structure in $Pb[B(Im)_4]X$ compounds and are expanding this work to different metals and borate structures as well as modifying the network through the identity of the intralayer counterion.

Acknowledgment. C.J.Z. acknowledges the Petroleum Research Fund (PRF No. 39625-G5M) and the University of Akron for faculty research grants (FRG-1524 and FRG-1565). We also wish to acknowledge NSF Grant CHE-

0116041 for funds used to purchase the Bruker-Nonius diffractometer and the Kresge Foundation and donors to the Kresge Challenge Program at The University of Akron for funds used to purchase the NMR instruments used in this work.

Supporting Information Available: Crystallographic information files (CIF). This material is available free of charge via the Internet at http://pubs.acs.org.

IC0497984